

# Reverse Optical Probing (ROPING) of Neocortical Circuits

GLOSTER AARON\* AND RAFAEL YUSTE

HHMI, Department Biological Sciences, Columbia University, New York

**KEY WORDS** imaging; calcium; synapse; confocal

**ABSTRACT** We describe an optical technique to detect circuits of synaptically connected neurons. By combining calcium imaging of the spontaneous activity of neuronal populations with intracellular recordings from a given neuron, we perform a type of reverse correlation analysis to detect neurons that generate action potentials time-locked to the synaptic currents of the recorded cell. This technique can quickly reveal monosynaptically connected neurons. **Synapse 60:437–440, 2006.** © 2006 Wiley-Liss, Inc.

## INTRODUCTION

We introduce our technique, named ROPing (**R**everse **O**ptical **P**robing), that uses fluorescent calcium indicators to detect synaptic connections. Specifically, the technique identifies those neurons in a brain slice that most often fire an action potential (AP) *before or coincidentally with postsynaptic currents (PSCs) recorded from a single neuron*; the idea is that those neurons firing before or at the same time of a PSC in a single recorded neuron are likely to be synaptically connected or share common inputs with that recorded neuron. In contrast to previous optical techniques (Kozloski et al., 2001; Peterlin et al., 2000), ROPing does not require stimulation of neurons; rather, passively recording the spontaneous activity of the slice is enough to reveal potential connections.

ROPing holds great promise for finding synaptically coupled neurons, in either the forward or the reverse direction. Although detecting connected pairs of neurons can be achieved by randomly patching neurons that are near-neighbors, there are scant dual intracellular recordings performed between synaptically coupled neurons that are located further from each other, between different layers, or between different cortical areas or different brain regions. ROPing can be in principle applied to pursue this goal, particularly after improving the system with longer acquisition durations, faster frame acquisition rates, and faster computation speeds.

## MATERIALS AND METHODS

### Electrophysiology

PND 18–22 C57Bl/6 mice were anesthetized and 350  $\mu$ m coronal slices were cut on a vibratome (Leica). Slices were transferred to warm (37°C), oxygenated,

ACSF (3 mM MgSO<sub>4</sub>, 1 mM CaCl<sub>2</sub>), and allowed to equilibrate to room temperature. Whole-cell recordings in V1 were performed using 6–9 M $\Omega$  pipettes, filled with (mM): 130 K-methylsulfonate, 11 biocytin, 10 KCl, 10 HEPES, 5 NaCl, 2.5 Mg-ATP, 0.3 Na-GTP. Recordings were performed in a warmed (34°C), oxygenated conventional ACSF (1 mM MgSO<sub>4</sub>, 2 mM CaCl<sub>2</sub>, 3 mM KCl) with Axopatch 200B (Axon Instruments) and a BVC-700 (Dagan Instruments) amplifiers and digitized with an A/D board (Instrutech) using Igor (Wavemetrics) on the electrophysiology computer (Macintosh, see Fig. 1). Large layer 5 pyramidal neurons were selected as the trigger cells, identifiable with infrared DIC optics.

### Imaging

We prepared a 100- $\mu$ l solution containing: 50  $\mu$ g of fura-2AM, 2  $\mu$ l pluronic acid, 48  $\mu$ l DMSO, and 50  $\mu$ l ACSF. This solution was divided among four cortical slices and directly applied via pipette to the cortex of each slice carefully and under visual guidance so that the solution could be seen to collect over the cortices. The slices were then left undisturbed in darkness for 1 h. For each pixel, we defined the fluorescence change over time as  $\Delta F/F = (F_1 - F_0)/F_0$ , expressed in %, where  $F_1$  is fluorescence at any time point, and  $F_0$  is fluorescence at the beginning of each trial.

\*Correspondence to: Gloster Aaron, Biology Department, Wesleyan University, Middletown, CT 06458. E-mail: gaaron@wesleyan.edu

Contract grant sponsors: National Eye Institute and the Kavli Institute of Brain Science.

Received 11 January 2006; Accepted 15 June 2006

DOI 10.1002/syn.20316

Published online in Wiley InterScience (www.interscience.wiley.com).

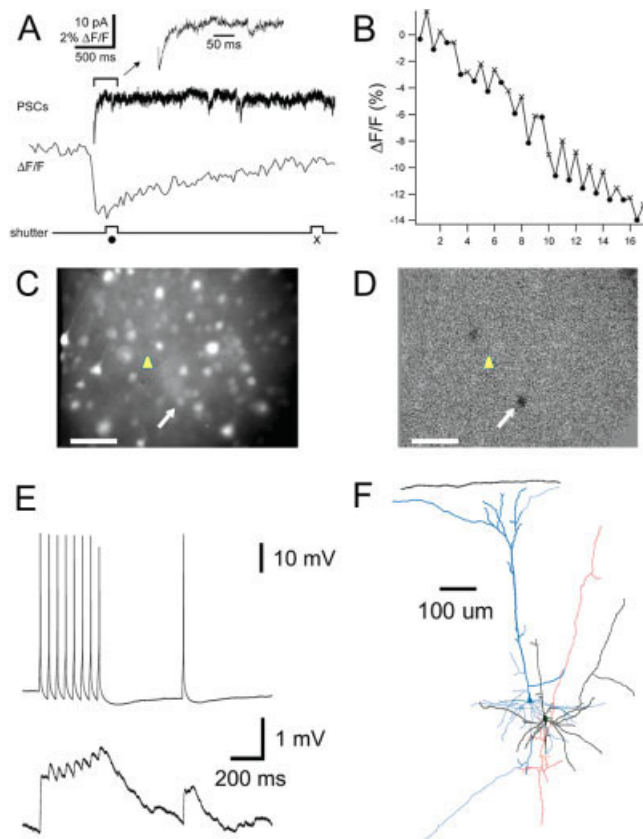


**Fig. 1.** ROPing with a video camera. **(A)** Large amplitude spontaneous PSCs (top trace) opens a fast camera shutter and triggers the image-acquisition system. A blowup of the PSC is shown above, as indicated by the arrow. A somatic calcium transient caused by an action potential in the presynaptic cell (middle trace, representative example from a different experiment) outlasts the PSC itself so that its peak can be detected within 200 msec of the peak of the action potential. This transient is measured by the change in fluorescence ( $\Delta F/F$ ), and the fluorescence is quenched by calcium, yielding a darkening of the imaged neuron. The shutter is opened by the triggering PSC (bottom trace), illuminating the slice with UV light for 150 ms, capturing an image. This PSC-triggered shutter opening is designated as the “ON” trial, and is symbolized by a dark circle in subsequent figures. After 2.5 s, an “OFF” trial is taken, symbolized by an “X.” “OFF” frames are subtracted from “ON” frames, yielding a relatively dark spot in the image of the slice for those neurons that fire an action potential at the same time (or  $\sim 1$  s before) as the triggering PSC. **(B)**  $\Delta F/F$  of the ROPed neuron for each ON and OFF trial, where each ON trial is indicated by a filled circle. The y-axis represents the change in fluorescence intensity. Note that in 12 of 17 PSC-triggered ON–OFF pairs, the ON trial was darker (less intensity) than the OFF trial, indicative of an AP occurring in that neuron during the ON trial. **(C)** Fluorescent image of the field of view (the electrode is invisible as it contains no indicator dye). The yellow triangle indicates the position of the triggering neuron, and the arrow points to the ROPed neuron. Scale bar = 50  $\mu\text{m}$ . **(D)** Subtraction map showing the average of all differences between ON–OFF trials. Each OFF trial is subtracted from the ON trial, yielding 17 images like those in Figure 2C, and then the mean of those 17 is depicted here. Dark pixels indicate regions where the average fluorescence differences between ON and OFF trials are largest. As in **(C)**, the triggering and ROPed neuron are indicated. **(E)** APs evoked in the ROPed neuron produce monosynaptic EPSPs in the trigger neuron, confirming a strong synaptic connection between these neurons. Each neuron was recorded in current clamp. The action potentials are from one representative trace, while the EPSPs are the average of 15 trials. **(F)** Reconstruction of the morphologies, with the trigger neuron in blue, the ROPed neuron in black, and the axon of the ROPed neuron in red. Both cells are pyramidal neurons, although the trigger neuron extends a branching apical dendrite to the pia surface, while the ROPed neuron displays more localized dendrites.

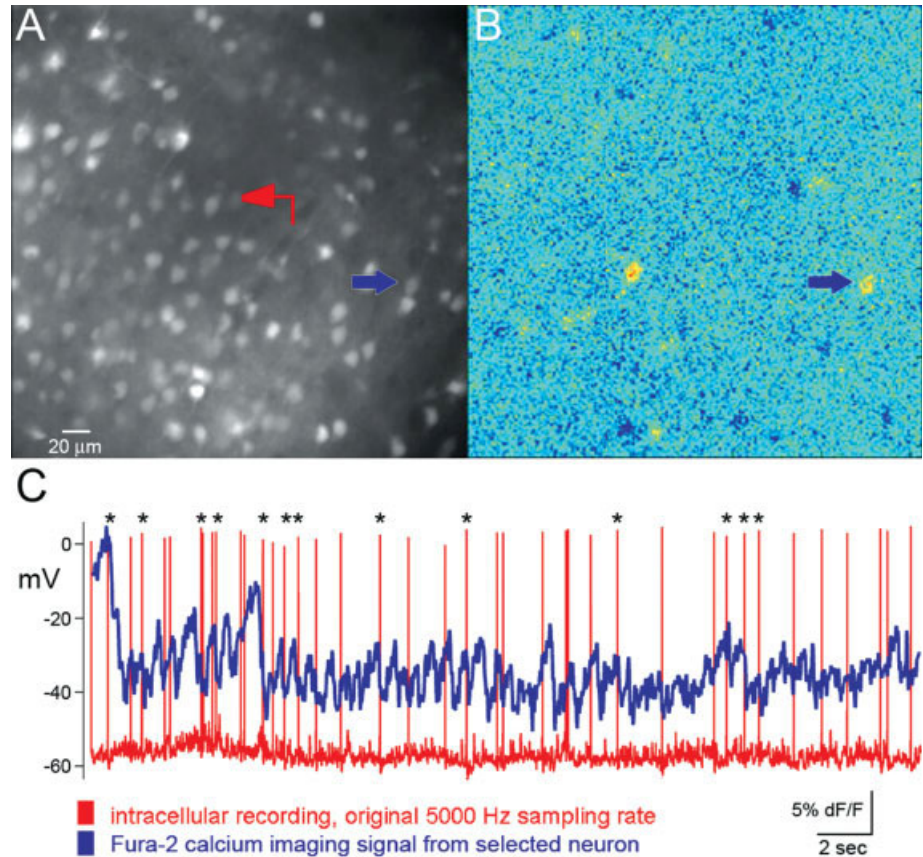
Images were collected with a SIT video camera (Dage) connected to an 8 bit frame grabbing board (Scion LG3) on the imaging computer (Macintosh). Frames were collected at 30 frames/s with a 40  $\times$ /0.8 noradrenaline objective (Olympus) and a 385-nm excitation filter (same system used in Kozloski et al., 2001). Control of ultraviolet illumination was performed with a Uni-Blitz model D122 shutter driver. Two sets of images, ON and OFF, were collected for each triggering PSC (Fig. 1). The ON image consisted of an average of five frames (1/6 s exposure) and imaging was triggered via a window discriminator (WPI). The OFF image, also an average of five frames, was triggered by the imaging computer with custom made macros in NIH image 1.6 software. A Master-8 (AMPI) was used to control the flow of triggering TTL pulses (Fig. 1).

In a second method using the same optics and excitation wavelength (Figure 2), images were collected continuously as large movies using a slit-disk spinning confocal unit (Olympus Disk-Scan Unit), a Hamamatsu C9100-12 CCD camera, and an acquisition program, SimplePCI (Cimaging). Whole-cell patch-clamped layer 2/3 pyramidal neurons in current clamp were recorded while simultaneously imaging for 30 s a 320  $\times$  320  $\mu\text{m}$  field of view with 256  $\times$  256 spatial and 36 frames/s temporal resolution. The 30 s of intracellular activity was then down-sampled from 5 kHz to 37 Hz to match the temporal resolution of the movie. Using a Matlab macro, the movie was then cross-correlated with the intracellular recording, pixel by pixel, using a standard covariance algorithm. After 15 min of computer processing time, a 256  $\times$  256 “correlation map” was produced. Given the shorter time allowed for collecting spontaneous activity with this method, we chose to increase the rate of spontaneous activity using a low divalent cation and slightly increased potassium ACSF (1 mM  $\text{Mg}^{2+}$ , 1.2 mM  $\text{Ca}^{2+}$ , 3.5 mM  $\text{K}^{+}$ ). Numerical results are presented as the mean  $\pm$  standard deviation, unless stated otherwise.

### ROPING CAN REVEAL SYNAPTICALLY CONNECTED CELLS

ROPing works by taking advantage of the direct correspondence between an AP in a neuron and the calcium transients in the somas of neurons labeled with the acetoxymethyl ester (AM) form of fura-2 (Smetters et al., 1999; Tsien, 1981; Yuste and Katz, 1991). While recording from a single neuron in whole-cell mode, single synaptic events such as PSCs or PSPs can be detected and their timing correlated with the optically detected AP activities of surrounding neurons in the slice (Fig. 1). Our first attempts to develop this technique were performed with a SIT camera as the imaging device. We experimented with continuous optical recording of the circuit activity to perform a traditional reverse-correlation protocol (Arieli et al., 1996; Dayan

Fig. 2. ROPing neurons with a confocal microscope. The activity of  $320 \times 320 \mu\text{m}$  area of cortex is recorded as a continuous movie at 36 frames/s while the intracellular activity of a single patched neuron is recorded. Neurons in this movie can be seen as groupings of white pixels in a fluorescent image of the field of view (A). The position of the patched neuron is indicated here with a triangle shape representing the patch electrode (the electrode is invisible as it contains no indicator dye). The fluorescent changes in each pixel of the movie ( $256 \times 256$  pixels) are cross-correlated with the intracellular recording, producing a correlation map (B), where colors toward the red indicate positive correlations and colors toward the blue indicate negative correlations. A relatively positively correlated neuron is indicated here with an arrow in both A and B panels. The fluorescent changes in this one neuron (in blue) are superimposed against the intracellular current clamp recording (in red) of the patched neuron (C). As shown, there is a strong correlation between significant fluorescent changes in the imaged neuron and spontaneous action potentials in the patched neuron (correlated events highlighted with \*).



and Abbott, 2001). However, such long-term imaging produces indicator bleaching and photodamage. Therefore, we employed a more practical method that takes advantage of the fact that the fluorescent signal dynamics associated with APs are themselves much longer in duration ( $>1$  s) than APs. Because the delays associated with the detection of the PSC and triggering the camera are small ( $<10$  msec) compared with the fluorescent signal dynamics, we can trigger a “snapshot” calcium image with a spontaneous PSC, illuminating the slice while the relatively long fluorescent transient from the AP is still detectable (Fig. 1A). A baseline image is then taken 2.5 s after the triggering event, and this baseline is subtracted from the average image taken during the transient, creating a subtraction map that should highlight *only* those cells that were active simultaneously with the PSC (Fig. 1D). All other activity in the movie should average out. Because of the long delay in the calcium decays, neurons that fire up to 1 s *before* the PSC occurred may also be detected, although the largest differences will be derived from those instances where the first image is most often triggered near the peak of the calcium signal. This is repeated up to 40 times for a typical experiment. To clarify the description of the experiments, we refer to the neuron from which we record the PSCs that

triggers the window discriminator as the *triggering* cell, and the neurons optically detected as the *ROPed* neurons.

We pursued this strategy in four experiments, patching pairs of neurons guided by the ROPing procedure. In the experiment illustrated in Figure 1, we detected two neurons that generated calcium transients systematically correlated with the EPSPs detected in the intracellular recording of the triggering cell (Fig. 1D). We chose the neuron with the stronger correlation (i.e., darker overall pixels) as the ROPed neuron. Establishing the dual recording, we found a strong excitatory synaptic connection between the ROPed neuron and the triggering cell (Fig. 1E), with a mean evoked EPSP amplitude of  $1.86 \pm 0.04$  mV. The short and relatively invariable latency from the peak of the AP to the beginning of the EPSP ( $1.4 \pm 0.03$  ms,  $n = 22$ ) demonstrated a monosynaptic connection between these two pyramidal neurons. This connection was also confirmed by the anatomical reconstruction of the neurons that showed the axon of the ROPed cell contacting the dendrites of the triggering neuron (Fig. 1F). In other experiments, direct synaptic connections were not detected, although we found correlated intracellular activity (common oscillations or common inputs) in the dual patch clamp recordings (data not shown).

### ROPING WITH A CONFOCAL MICROSCOPE

To improve on the power of ROPing, we realized a more sophisticated method that avoided bleaching through the use of a slit-disk confocal microscope. The benefit of this method is that better signal-to-noise is achieved from the signals originating in the plane of focus, allowing less light used to produce the signal. Imaging with less intense light produces less bleaching and photodamage. Thus, images can be recorded continuously, and, as frame rate acquisition increases, the temporal precision of this technique will also increase.

A potential disadvantage of this technique is that the confocal imaging reveals neuronal activities in an even more confined optical plane relative to regular fluorescence imaging and may therefore limit the number of neurons sampled. However, this disadvantage can be mitigated in future experiments by simply taking multiple movies at varying depths in the slice, thus gathering multiple optical sections for analysis. Another challenge introduced is the large size of the movie files acquired and the processing time required to produce a correlation map, but that challenge is mitigated as faster computers are produced. At present using a 2 GB RAM computer with 3 GHz processing speed, we can correlate every pixel in a 30 s movie ( $256 \times 256$  pixels) with the intracellular recording, producing a correlation map within 15 min where more red pixels are positively correlated with the intracellular activity, and more blue pixels are negatively correlated (Fig. 2B). While these correlation values are small (see below), that is to be expected given the fact that we are recording spontaneous activity: the PSCs recorded in a single neuron may originate from dozens to hundreds of neurons in the slice. Thus, a 0.1 correlation value (where 1.0 is a perfect correlation) may be considered very high under these circumstances.

We found compelling results from six out of eight different movies sampled, although this analysis was made offline, so the ROPed neuron was not patched. Results from one of these experiments are illustrated (Fig. 2). Each pixel in Figure 2B represents the value of a covariance function at the zeroth time lag. The mean pixel value was  $-0.004 \pm 0.03$  (mean  $\pm$  SD). The mean pixel value for the neuron indicated in Figure 2B was  $0.08 \pm 0.02$  (from a square of 9 contiguous pixels roughly representing the center of the neuron), significantly higher than the mean covariance value from all pixels ( $P < 0.01$ ). We were thus encouraged that this technique at least identified neuronal cell bodies (com-

pare Fig. 2A and 2B), demonstrating that some somata can produce a signal that is significantly detected over the random fluctuations of nearby pixels. Furthermore, by showing the mean fluorescent changes in the pixels comprising one of the positively correlated soma, it is seen that the intracellular activity of the patched neuron is correlated with the largest fluorescent changes from the ROPed soma (Fig. 2C).

There were two movies analyzed where no significant correlations could be found between the intracellular activity of one neuron and the fluorescent fluctuations in the movie (as assessed above). In five other movies we found results similar to those in Figure 2.

### FUTURE PROSPECTS

Roping could in principle be applied to systematically track neuronal circuits. By relying on a reverse correlation paradigm, and using window discriminators of different amplitudes and signs, it could be used to detect both excitatory and inhibitory connections and also to detect connections of different strength. Thus, it should be possible to optically dissect circuits in real time, with relatively accessible equipment, as demonstrated in Figure 1.

### ACKNOWLEDGMENTS

The authors thank the members of the laboratory for comments and Stuart Samuels for anatomical reconstructions. The authors also thank James Kozloski for the initial attempts to reverse correlate calcium imaging movies with intracellular recordings and Jason MacLean and Brendon Watson for help with experiments.

### REFERENCES

- Arieli A, Sterkin A, Grinvald A, Aertsen A. 1996. Dynamics of ongoing activity: Explanation of the large variability in evoked cortical responses. *Science* 273:1868–1871.
- Dayan P, Abbott, LF. 2001. *Theoretical neuroscience*. Cambridge: MIT Press.
- Kozloski J, Hamzei-Sichani F, Yuste R. 2001. Stereotyped position of local synaptic targets in neocortex. *Science* 293:868–872.
- Peterlin ZA, Kozloski J, Mao B, Tsiola A, Yuste R. 2000. Optical probing of neuronal circuits with calcium indicators. *Proc Natl Acad Sci USA* 97:3619–3624.
- Smetters DK, Majewska A, Yuste R. 1999. Detecting action potentials in neuronal populations with calcium imaging. *Methods* 18: 215–221.
- Tsien RY. 1981. A non-disruptive technique for loading calcium buffers and indicators into cells. *Nature* 290:527–528.
- Yuste R, Katz LC. 1991. Control of postsynaptic  $Ca^{2+}$  influx in developing neocortex by excitatory and inhibitory neurotransmitters. *Neuron* 6:333–344.